

## DETC2003/PTG-48000

### APPLICATION OF A MULTIAXIAL FATIGUE CRITERION FOR THE EVALUATION OF LIFE OF GEARS OF COMPLEX GEOMETRY

Leonardo Borgianni

Paola Forte

Luigi Marchi

University of Pisa, Italy  
Dipartimento di Ingegneria Meccanica,  
Nucleare e della Produzione,  
Via Diotisalvi 2, 56126 Pisa, ITALY  
Email: p.forte@ing.unipi.it

#### ABSTRACT

Gears can show significant biaxial stress state at tooth root fillet, due to the way they are loaded and their particular geometry. This biaxial stress state can show a significant variability in principal axes during meshing. Moreover loads may have non predictable components that can be evaluated with the aid of recorded data from complex spectra. In these conditions, commonly adopted approaches for fatigue evaluation may be unsuitable for a reliable fatigue life prediction.

This work is aimed at discussing a computer implementation of a fatigue life prediction method suitable for multiaxial stress states and constant amplitude or random loading. For random loading a counting procedure to extract cycles from complex load histories is discussed. This method, proposed by Vidal et al., is based on the r.m.s. value of a damage indicator over all the planes through the point where the fatigue life calculation is made. Miner's rule is used for the evaluation of the overall damage. The whole fatigue life of the component is evaluated in terms of the numbers of repetitions of the loading block.

FEM data are used to evaluate stresses under load. The implementation was validated using test data found in the technical literature. Examples of applications to gears are finally discussed.

#### INTRODUCTION

Among the possible causes of failure of a gear, bending fatigue is the most frequent [1]. The classical bending failure is characterized by the rise of a surface crack at about the middle of the tooth fillet, on the loaded side, where the tension stresses are higher.

Reasonably assuming that the gear works in the elastic range, fatigue life prediction is based, as for any other component, on the evaluation of the stress levels in particularly stressed points. Lewis' analysis (1892) is still at the basis of the standards for stress evaluation at the tooth root. In the literature many methods are proposed to calculate the maximum stress at the tooth root fillet, as function of the gear geometry and the applied load. In particular AGMA has developed standards for the evaluation of stress in different kinds of gears, spur, helical and bevel gears. Though these calculated stress values may be inaccurate, nevertheless they are a useful means to compare different solutions in the design stage. The stress value can be also compared to an allowable value below which there will be no gear failure for a given number of load cycles.

The procedure for fatigue life prediction is completed by the definition of the load spectrum, by the cycle counting and by the evaluation of the overall damage by charging a fraction of it to each fatigue cycle.

The success of a gear in the design stage is related to the availability of valid analytical models and standards for the prediction of stress in the tooth fillet and of experimental data or fatigue S-N curves obtained for similar gears and as function of material properties and quality, surface treatment, technological process and failure probability.

For gears the uniaxial fatigue assumption is only a rough approximation, acceptable only in the case of uniform tooth cross section and uniform load distributed on the tooth length. Actually even in such conditions the stress state is multiaxial and the fillet edge stress state is different from the fillet center stress state and the procedures for uniaxial fatigue life prediction applied to complex stress cycles can overestimate the component strength in operating conditions.

As gears with a more complex geometry are concerned, as face gears, the previous assumptions are even less sustainable because of the load distribution, generally not uniform and variable during meshing.

In order to overcome the limits of a uniaxial analysis since the mid 20's extensive studies have been undergone aimed at providing reliable design tools to deal with time dependent multiaxial stress states, but in spite of the numerous criteria developed up to now there is no universally acknowledged approach.

Restricting our survey to the methods regarding high cycle fatigue since gears are generally designed to last long, the first approach proposed for modeling multiaxial fatigue behavior is based on static rupture criteria, transforming the multiaxial stress state in an equivalent uniaxial stress yielding the same fatigue life. The most popular methods are based on Tresca's and von Mises' criteria, in which the static values of the principal stresses are substituted by their amplitudes and the yield strength is substituted by the uniaxial endurance limit. However it has been observed experimentally that the type of loading considerably affects the component fatigue behavior [2]. Moreover, those approaches don't take into account the effect of the sign of the average stress and the different influence of mean shearing and normal stresses.

The criteria presently used to deal with the more general cases of multiaxial stress and non-proportional loading can be divided in three main groups: those based on the critical plane approach, those based on the stress invariants and finally those based on the average stress inside an element volume. In the first case, the fatigue damage evaluation is accomplished on a particular plane, called critical, where the amplitude or value of some stress components, or a combination of them, reaches the maximum value [3-6]. In the second case the components involved in these models are the hydrostatic stress and the quadratic invariant of the stress deviator, a combination of which is compared with an allowable value [7-9]. These methods however don't give any information about the orientation of the potential fracture. Finally, in the last case, the fundamental quantities are average normal and shearing stresses acting on a plane inside an element volume [10]. There are also criteria that combine the characteristics of the above mentioned ones [11].

The multiaxial fatigue life prediction method adopted in this work is that proposed by E. Vidal et al. [12] based on the critical plane approach, successfully employed and validated by Centro Ricerche Fiat [13]. The method includes proper experimental dependence (the mean shearing stress has no effect on fatigue life while on the contrary the mean normal stress has a considerable influence) and a correct definition of the shearing stress amplitude by using the loading path on the shearing stress plane [6]. The criterion has been applied using a series of finite element analyses which gives the stress distribution in the tooth fillet all through a meshing cycle.

## THE MULTIAXIAL FATIGUE CRITERION

By using Vidal's method it is possible to predict the fatigue life of a component in HCF conditions, if the material fatigue characteristics are known by means of S-N alternating fully reversed bending, alternating fully reversed torsion and zero to max bending curves, and once the map of the components of the stress tensor is obtained by FEM analyses.

The method takes into account the possibility that the principal axes rotate, even significantly, thus activating different sliding planes; for that reason damage is calculated for every plane passing through the considered point. Considering a plane  $h$ , the plane damage indicator can be expressed as:

$$E_h = \frac{1}{\sigma_{-1}(N)} \left[ a(N) \max \|\bar{\tau}_{ha}(t)\| + b(N) \max \sigma_{ha}(t) + d(N) \sigma_{hm} \right] \quad (1)$$

where  $a(N)$ ,  $b(N)$ ,  $d(N)$  are parameters which depend on the material fatigue characteristics.  $\sigma_{-1}(N)$  is the alternating fully reversed bending endurance limit at cycles  $N$ .  $\tau_{ha}$  is the shearing stress amplitude defined as the vector difference between the shearing stress  $\tau_h$  at time  $t$  and the mean shearing stress  $\tau_{hm}$ , on plane  $h$ . The latter is calculated as the distance between the considered point and the center of the smallest circumference inscribing the loading path traced by vector  $\tau_h$  on plane  $h$  during a cycle.  $\sigma_{ha}$  and  $\sigma_{hm}$  are the mean normal stress and normal stress amplitudes in a cycle.

The total damage is estimated by means of an integral average of the damage of all planes:

$$E_{FB} = \sqrt{\frac{1}{4\pi} \int_S E_h^2 ds} \quad (2)$$

Fatigue failure after a specific number of cycles arises when  $E_{FB}=1$ .

The relative complexity of the method may be faced with the presently available computing means.

Although the method is devised to predict the fatigue life of a component subjected to a constant amplitude cyclic load, it can be extended to estimate fatigue life in case of random loading.

## THE NUMERICAL PROCEDURE

A code implementing the chosen fatigue life prediction method has been developed in a Mathcad 2001 environment, optimized to be run on a PC with a reasonable computing time.

The input is a complex load history defined by means of the stress tensor in different instants and the material fatigue characteristics.

The load history is sampled as a series of static conditions, for which it is possible to determine the stress distribution by a FEM analysis. That means entering a matrix  $[m \times 6]$ , where  $m$  is the number of nodes times the number of load conditions and 6 is the number of components of the stress tensor.

As regards the material fatigue characteristics it is necessary to have the three S-N curves corresponding to alternating fully reversed bending, alternating fully reversed torsion and zero to max bending, obtained from standard smooth specimen tests. It is also necessary to correct the experimental curves in order to consider not only the initiation of cracks but also their propagation. The correction at high cycles is made by means of a fictitious slope intermediate between the zero slope and the experimental one below  $10^6$  cycles. Since this approach is tuned for the hard metals, for which the ratio of the alternating bending and torsion endurance limits ranges from 0.577 to 0.8, the alternating bending and torsion curves cannot have different corrected slopes.

Generally S-N curves are given with a 99% reliability but in the code it is possible to obtain higher or lower reliability S-

N curves by using a correction parameter which substantially raises or lowers the curves. It is also possible to modify the curve with a surface finish factor which depends on the material tensile strength.

The method requires that damage is calculated on every plane through the considered point  $O$ , but it is convenient to choose a finite number of planes and the evaluation will be done by means of a finite summation instead of an integration:

$$E_{FB} = \sqrt{\frac{1}{4\pi} \sum_{h=1}^n E_h^2 \Delta s} \quad (3)$$

To do that the unit vectors normal to the sliding planes  $h$  must be distributed uniformly in the whole space and the value of area  $\Delta s$  must be defined. The set of these vectors covers a sphere which has been discretized with angles  $\Delta\theta$  and  $\Delta\varphi$  of  $10^\circ$  corresponding to considering 614 points on its surface and 614 planes (Fig.1).

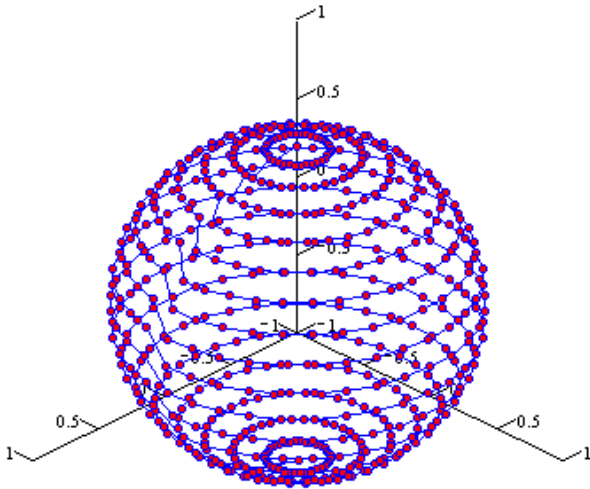


Figure 1 - Discretized sphere

In the generic point  $O$  the stress vector can be expressed by the stress tensor  $T$  and the direction cosines of the unit vector  $h$ ,  $(h_1, h_2, h_3)$ , normal to the plane. The normal and shearing components of the stress vector can be defined in a Cartesian coordinate system, one axis of which is parallel to  $h$  and the other two,  $hort_1$  e  $hort_2$ , lie on the plane:

$$\sigma = T \cdot h \cdot h \quad \tau_1 = T \cdot h \cdot hort_1 \quad \tau_2 = T \cdot h \cdot hort_2 \quad (4)$$

The parameters  $a(N)$ ,  $b(N)$  and  $d(N)$  of Eq.(1) can be evaluated from fatigue tension-compression and torsion test data for a smooth specimen, substituting the stress values in the equation of damage and obtaining a system of non-linear equations. Solving such system yields explicit expressions of  $a(N)$ ,  $b(N)$  and  $d(N)$  and also indicates the validity range of the model, which turns out to be

$$\frac{1}{\sqrt{3}} < \frac{\tau_{-1}(N)}{\sigma_{-1}(N)} < \frac{\sqrt{3}}{2} \quad (5)$$

In order to predict fatigue life of a component subjected to multiaxial stress and to a random load history it is necessary to identify a suitable stress parameter to which cycle counting can be applied.

As cycle counting parameter Vidal et al. propose to use the projection,  $V(t)$ , of the octahedral tangential stress on a line lying on the deviatoric plane, passing through the origin, and

whose orientation is defined by angle  $\psi$  (Fig2). Counting can be done for a reasonable number of  $\psi$ , and each  $\psi$  will be related to a counted history and therefore to a certain damage. Among the set of calculated solutions the one corresponding to maximum damage is considered. As the number of considered angles increases, accuracy of the final result increases as well as computing time.

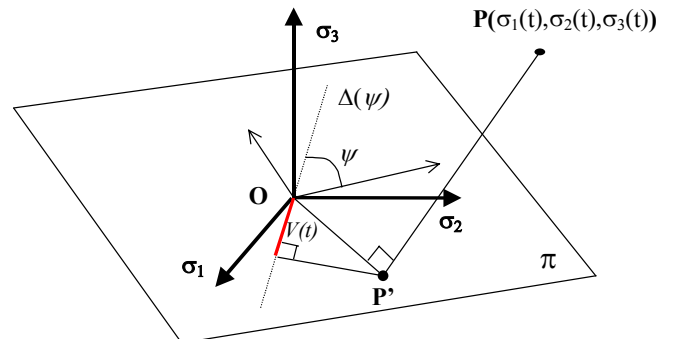


Figure 2 - Definition of  $V(t)$

Once the counting parameter is chosen, the cycles are counted by a rainflow counting method. The loading history expressed by  $V(t)$  is first reduced to a series of peaks and valleys and then counted, reducing the complex load history of the counting variable into a number of cycles. Then the damage selected criterion is applied to each cycle and overall damage is estimated by Miner's linear damage rule.

The procedure adopted for the calculation of life to failure includes two steps:

1. For every amplitude of  $V(t)$ ,  $E_h$  and  $E_{FB}$  are calculated for a discrete number of cycles,  $N$ , then the entire function  $E_{FB}(N)$  is interpolated (Fig.3); for every load level, life to failure corresponds to the value of  $N$  for which  $E_{FB}$  equals to 1.

2. The linear damage rule is applied considering all cycles counted by the rainflow method. Therefore total damage is:

$$D = \sum_1^{\text{cycle no.}} \frac{1}{N_{crit}} \quad (6)$$

and life to failure is

$$N_{failure} = \frac{1}{D} \quad (7)$$

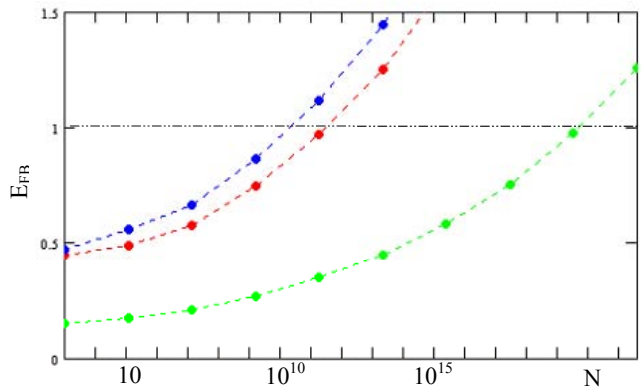


Figure 3 - Global damage as function of  $N$  for different amplitudes of the counting parameter

The parameters which have influence on the results are:

- a) the S-N curves and their correction for high cycles;
- b) the accuracy of the calculated stress distribution, that is the

- mesh fineness, the number of considered load conditions, the accuracy of load and constraint conditions;
- c) the interpolation of  $E_{FB}(N)$ ;
- d) the number of  $\Delta\psi$ ;
- e) the number of planes for which damage is calculated.

The choice of the above parameters is obviously a compromise between the required accuracy and the available computing resources.

### THE NUMERICAL AND EXPERIMENTAL VALIDATION

The results obtained by the code implementation in Mathcad have been compared to the numerical results obtained by Vidal et al. [12]; unfortunately no details were available on the kind of assumptions and simplifications adopted in their fatigue code.

Figure 4 shows the test results of fully reversed and zero to max axial loading and fully reversed torsion for hollow cylindrical specimens. The diamonds indicate the fatigue life values predicted by Vidal et al. while the dots indicate the values obtained by the present authors. The close agreement of the two sets of results proves the validity of the model implementation.

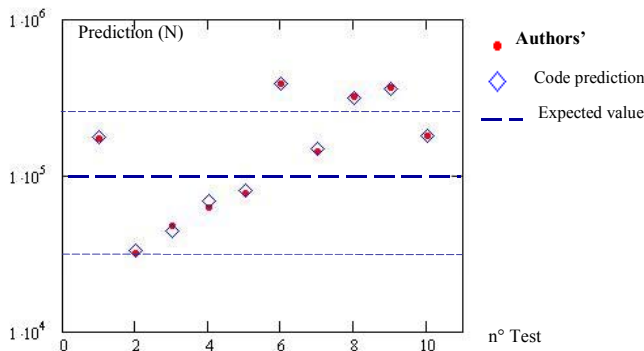


Figure 4 - Comparison of numerical and experimental results

Since presently there was no possibility of having our own experimental results, the method was validated on known cases available in the technical literature.

First of all the numerical results were compared with the experimental data reported in [12]. The specimens, made of heat treated carbon steel Ck45, are circular tubes with inner diameter of 32 mm and 1.5 mm thickness, loaded in two ways: inner pressure combined with axial loading and combined axial and torsion loading.

In Fig.4 the life extrapolated from experimental data and the range of scattering of  $\pm 3$  times that value are also reported to be compared with the numerical ones. The numerical values are within or very close to the range of scattering.

In order to compare the values predicted by the implemented method with experimental results from independent sources, the data from an experimental campaign reported in [14] were used.

The specimen material is normalized steel AISI 1045 (0.44% C, 0.7% Mn, 0.23% Si), with an ultimate tensile strength  $S_u$  of 621 MPa and yield strength  $S_{0.2}$  of 380 MPa. The specimens are notched cylinders subjected to torsional and bending loads. The S-N curves corresponding to alternating torsion and axial loading are given with a reliability of 99%. The zero to max ( $R=0$ ) torsion curve was obtained using

Goodman's criterion. The curves were shifted by a correction coefficient to lower strength values, to bring them to a reliability condition of 50%, assuming a Gauss distribution for fatigue strength values.

The specimens were subjected to combined in-phase fully reversed torsion and bending loads. The specimen was modeled and a FEA carried out. The numerical tests were done with a negligible computing time adopting the following parameters: 266 planes,  $\Delta\psi=30^\circ$ , number of cycles at which the damage curve is defined [ $10^4$   $10^5$   $10^6$   $10^7$   $10^9$ ]. In Fig.5 the predicted values are compared with the experimental ones and with Von Mises predictions. Results from the multiaxial method are in good agreement with experimental data, while the Von Mises predictions show a non conservative behavior.

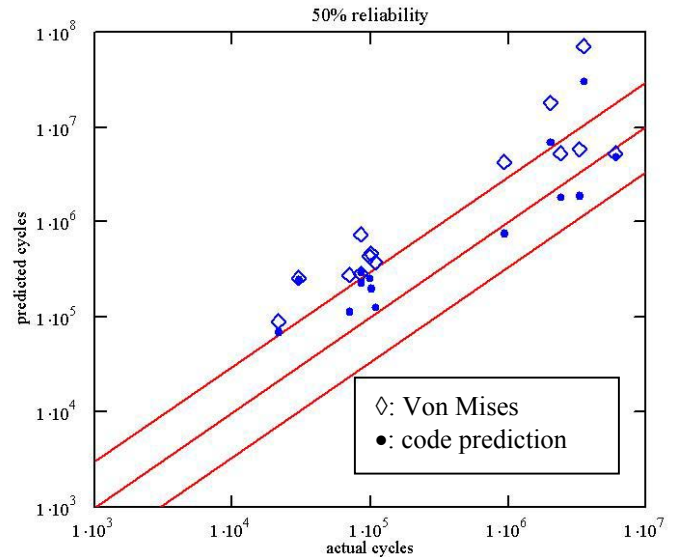


Figure 5 - Comparison of predicted and actual cycles for notched specimen

### APPLICATION TO GEARS

The method was finally applied to bending fatigue life prediction of unconventional gears in order to find possible shortcomings. Such application has required a complex preliminary work of FEM modeling and simulation.

The solid modeling and FEA of complex gears are described in a previous work [16]. If gears have a complex geometry as face gears do the tooth surfaces are generated by envelopment by means of an originally developed code [17] as sets of points which the CAD 3D system Pro/ENGINEER 2000i uses to create the solid models of the two meshing teeth. More common geometry teeth can be created directly in the CAD environment. From the CAD model, in IGES format, the pre-processor of the FE code Ansys generates the FE models. The mesh of Fig.6 has been obtained by extruding a mesh generated on the tooth front surface. The extruded mesh is also constrained by mapped meshes created on the lateral surfaces of the solid. This procedure enables mesh controls (element size and number of nodes) to be performed acting directly on the mesh of the lateral surfaces where contacts occur. The mesh is clearly more regular than in the previous case yielding more accurate results. This is due to the more advanced and flexible tools available in FEM pre-processors.

With advanced CAD systems, such as the one used, the operating conditions can be simulated properly placing the solid models of the gears according to their relative angular positions during meshing. Considering toothed sectors it is convenient to model in the CAD environment only two meshing teeth and create the remaining parts of the FEM model copying nodes and elements of that single pair around the wheel axes. Considering toothed sectors it is convenient to model only one pair of meshing teeth in the CAD environment and to generate the rest of the FEM model copying nodes and elements of that pair around the wheel axes.

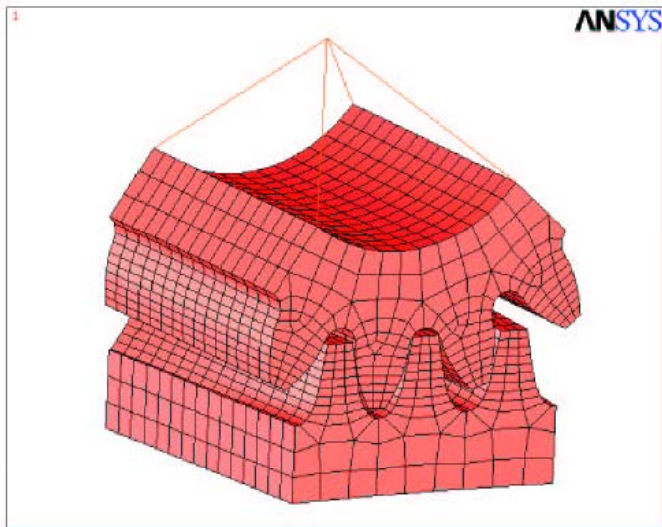


Figure 6 - FEM model of meshing pinion and face gear sectors

To make the modeling of the tooth contact more realistic and to evaluate the gear behavior more accurately a non linear analysis is necessary. Ansys is a software provided with algorithms to automatically detect contact conditions between bodies. In particular, once the tooth volume is meshed, contact elements are defined on the active flank of the tooth to simulate meshing conditions. Because of the non linearities typical of contact problems, the code converges to solutions after a few iterations solving a series of linear problems corresponding to the steps of load application gradually increasing up to the final value. Convergence is reached if the first trial linear solution is close to the exact one and it is strictly related to the mesh dimension in the contact area which should be fine enough to guarantee the gradual load transmission from one body to the other.

The FEM analysis was performed on a face gear sector completely constrained on the rim and side surfaces while the nodes of the side surfaces of the pinion are constrained to rotate rigidly around its axis. The load was applied as a constant torque acting on a node on the pinion axis.

A numerical test campaign has been carried out considering the sectors in different relative positions in the theoretical meshing process. The stress history of the meshing teeth fillets has thus been reproduced. A limitation of the described analyses is that they are based on static evaluations, that is they neglect dynamic effects which can affect the load level and also the location of the most critical points, the load distribution among teeth and the dynamic behavior of the entire power drive. This problem can be faced accomplishing

dynamic instead of static analyses, for example with a dynamic explicit code.

The method was applied to a face gear drive with the following data. A 23 teeth pinion engaging a 143 teeth face gear were considered, with a  $25^\circ$  pressure angle, and a module of 2.8 mm. The pinion pitch diameter was 64.4 mm, with a face width of 42.6 mm, while the face gear had a 367 mm inner diameter and a 450 mm outer diameter. The models refer to three tooth gear segments in order to account for all the contacting teeth during meshing. A torque of 811 Nm was applied to the pinion.

The complete model was made of about 22000 hexahedral 8-node elements each having 24 degrees of freedom and 400 surface elements for each contact surface. Even if the mesh of the tooth root is rather coarse the number of nodes is sufficient for a rough prediction of the fillet areas more subjected to fatigue.

The FEA produced the stress tensor as function of time, for the nodes of a grid on the tooth root fillet of both the pinion and the face gear; in Fig.7 the stress components of two nodes located in the middle of the fillets are reported.

Comparing the stress plots for the two teeth a more uniform distribution is shown by the pinion node probably due to the pinion more regular shape.

The procedure described above for multiaxial fatigue life prediction was applied. The load history, expressed by the stress tensor in the fillet nodes of the two mating teeth, was sampled by 9 instants (11 considering zero load entrance and exit instants); the considered nodes were 198 for the pinion (22 columns x 9 rows for an almost rectangular grid) and 105 for the face gear (21 columns x 10 rows).

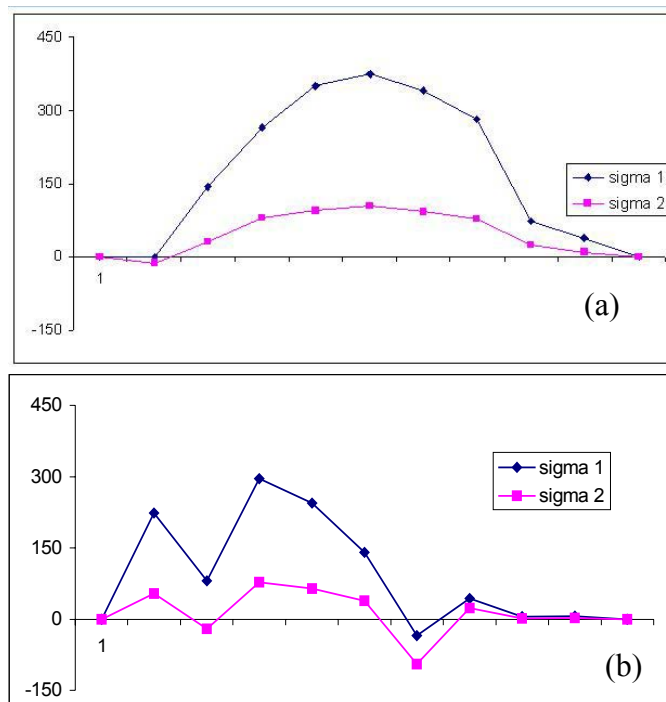


Figure 7 - Evolution of principal stresses [MPa] for a node of the tooth root fillet of pinion (a) and face gear (b) during meshing

Since the fatigue characteristics are not specifically known, approximate S-N curves based on ultimate static strength (1172

MPa) were used, modifying the slope of the curves according to the fictitious slope of the alternating torsion curve.

As for the parameters affecting the final results, after a convergence study, the following values were chosen as they represented the best compromise between computing time and solution accuracy: 266 planes for which damage is calculated,  $\Delta\psi=30^\circ$ , five points for the damage curve [ $10^6$   $10^7$   $10^8$   $10^9$   $10^{12}$ ]. With a high level PC (Pentium IV 2400 MHz) the calculation required 11.4 sec per node for a total time of 20 minutes.

In Fig.8 the damaged areas can be seen; The damage distribution is rather regular in the fillet longitudinal direction for the pinion tooth while it extends also on the face gear tooth flank direction. For this load condition and geometry the pinion appears to be more prone to damage in agreement with common practice. In fact its most stressed node has a predicted life of  $2.87 \cdot 10^8$  cycles while the most stressed node of the face has a predicted life of  $8.73 \cdot 10^8$  cycles.

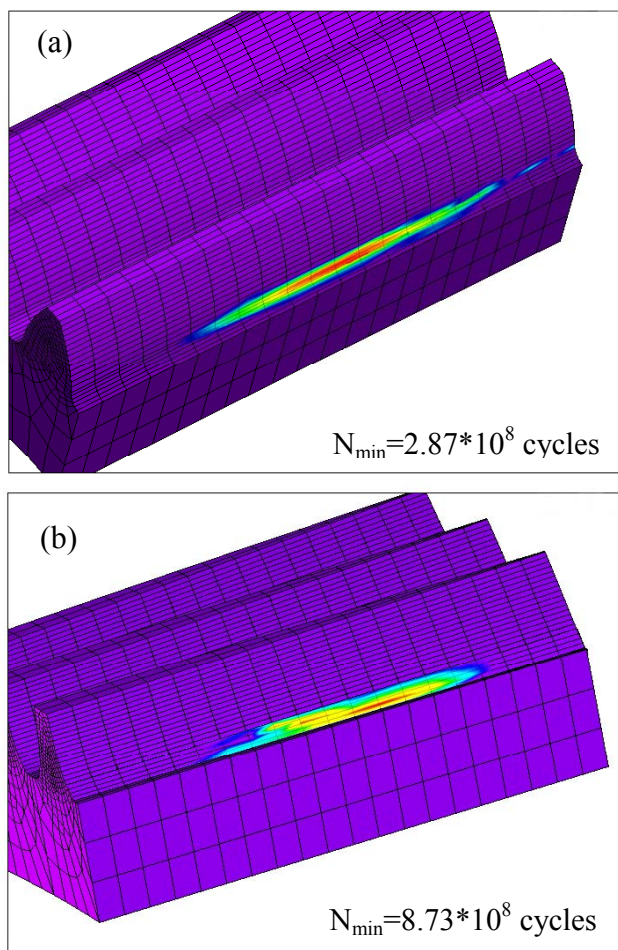


Figure 8 - Damage maps on the tooth root fillet of pinion (a) and face gear (b)

## CONCLUSIONS

In this paper a numerical procedure based on a calculation procedure for high cycle fatigue life prediction for a component subjected to multiaxial random loading has been presented. The method is particularly tuned for the hard metals, the most widely used in industrial applications. The presently obtained

results are quite close to those obtained by the authors of the method, thus proving the correct development of the numerical procedure.

As far as the software code is concerned, it was developed with the objective of minimizing the required computing resources, and as a matter of fact good results have been obtained even for complex load histories on a medium level PC.

The tests carried out to validate the criterion with experimental data obtained by other researchers has given satisfactory results showing a good correlation between predicted and real data.

The method was finally applied to a face gear. Even if the results presently are not validated experimentally they can give useful indications. A FEA test campaign could show the influence of geometrical factors and load conditions on the damage distribution at the tooth root fillet.

## REFERENCES

- 1 Alban, L. E., 1984, "Number 1 Gear failure Tooth Bending fatigue", SAE Tech Paper 841088.
- 2 Socie, D.F., et al., 1987, "Mixed mode small crack growth", *Fatigue Fract. Engng. Mater. Struct.*, **10** (1), pp. 1-16.
- 3 Findley, W. N., 1959, "A theory for the effect of mean stress on fatigue of metals under combined torsion and axial load or bending", *Trans. ASME, Series B*, **8**, pp. 301-306.
- 4 Matake, T., 1977, "An explanation on fatigue limit under combined stress", *Bulletin JSME* **20**, pp. 257-263.
- 5 McDiarmid, D.L., 1991, "A general criterion for high cycle multiaxial fatigue failure", *Fatigue Fract. Engng. Mater. Struct.*, **14**, pp. 429-453.
- 6 Dang Van, K., 1993, "Macro-micro approach in high cycle fatigue criterion", ASTM STP 1191, American Society for Testing and Materials, Philadelphia, pp. 120-130.
- 7 Sines, G., 1959, *Metal fatigue*, McGraw-Hill, New York.
- 8 Fuchs, H. O., Stephens, R. I., 1980, *Metal fatigue in Engineering*, John Wiley and Sons, New York.
- 9 Crossland, B., 1956, "Effect of large hydrostatic pressures on the torsional fatigue strength of an alloy steel", *Proc. Int. Conf. on Fatigue of Metals*, Inst. Mech. Engrs, London, pp. 138-149.
- 10 Grubisich, V., Simburger, A., 1976, "Fatigue under combined out-of-phase multiaxial stresses", *Proc. Int. Conf. Fatigue Testing and Design*, Society of Environmental Engrs., London, pp.271-278.
- 11 Papadopoulos, I.V., 1994, "A new criterion of fatigue strength for out-of-phase bending and torsion of hard metals", *Int. Journal of Fatigue*, **16**, pp. 377-384.
- 12 Vidal, E., et al., 1996, "Fatigue life prediction of components using multiaxial criteria", *Multiaxial Fatigue and Design*, ESIS 21, A. Pinneau et al. eds., London, pp. 365-378.
- 13 Blarasin, A., Giunti, T., 1997, "PRINCE: a software code for an integrated durability analysis", SAE Technical Paper 970710.
- 14 Kurath, P., 1989, "Summary of non-hardened notched shaft round robin program", *Multiaxial Fatigue*, G.E. Leese and D. Socie eds., SAE AE-14, pp.13-31.
- 15 AAVV, 1977, *Fatigue under complex loading*, Advances in Engineering Series, **6**, SAE.
- 16 Barone, S., et al., 2002, "CAD/FEM procedures for

stress analysis in unconventional gear applications”, *Int. J. of Computer Applications in Technology*, **15**(4/5), pp. 157-167.

17 Carmone, C., et al., 2001, “Analisi geometrica e cinematica di face gears ingrananti con pignoni a dentatura elicoidale”, XV Congresso AIMETA, Taormina 26 – 29 Settembre.